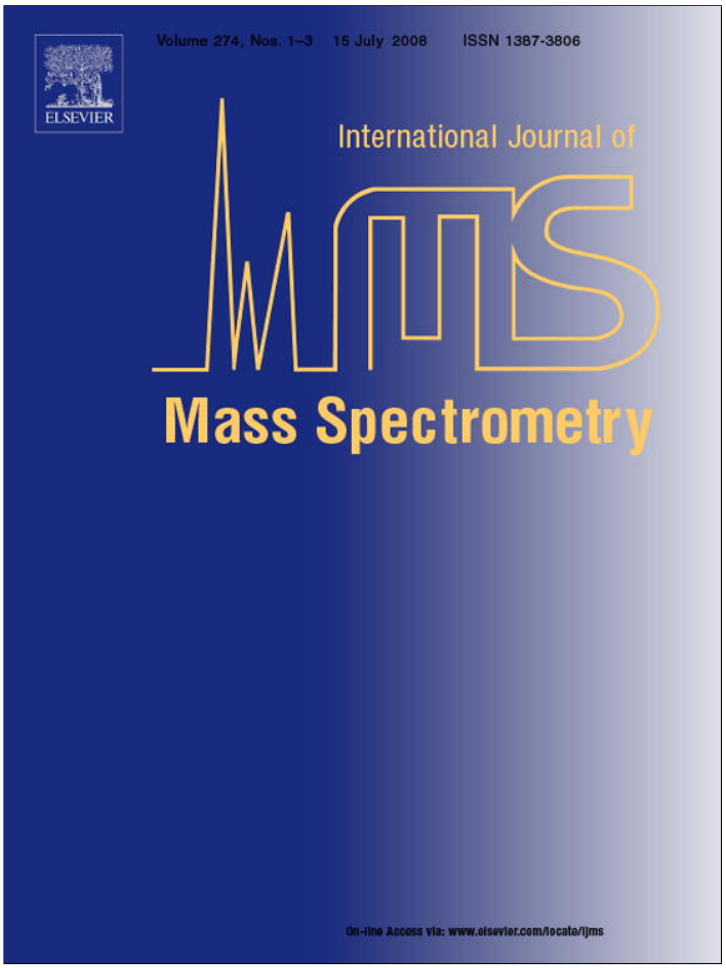

International Journal of Mass Spectrometry 274 (2008) 56–63

Contents lists available at ScienceDirect

International Journal of Mass Spectrometry

journal homepage: www.elsevier.com/locate/ijms

Analysis and differentiation of mineral dust by single particle laser mass spectrometry

Stephane Gallavardin*, Ulrike Lohmann, Daniel Cziczo[1]

Institute for Atmospheric and Climate Science, ETH Zurich, CH-8092 Zurich, Switzerland

ARTICLE INFO

Article history:
Received 5 February 2007
Received in revised form 28 April 2008
Accepted 30 April 2008
Available online 9 May 2008

Keywords:
Aerosol mass spectrometry
Mineralogy

ABSTRACT

This study evaluates the potential of single particle laser desorption/ionization mass spectrometry for the analysis of atmospherically relevant mineral dusts. Samples of hematite, goethite, calcium carbonate, calcium sulfate, silica, quartz, montmorrillonite, kaolinite, illite, hectorite, wollastonite and nephelinsyenit were investigated in positive and negative ion mode with a monopolar time-of-flight mass spectrometer where the desorption/ionization step was performed with a 193 nm excimer laser ($\sim 10^9$ W/cm^2). Particle size ranged from 500 nm to 3 μm. Positive mass spectra mainly provide elemental composition whereas negative ion spectra provide information on element speciation and of a structural nature. The iron oxide, calcium-rich and aluminosilicate nature of particles is established in positive ion mode. The differentiation of calcium materials strongly relies on the calcium counter-ions in negative mass spectra. Aluminosilicates can be differentiated in both positive and negative ion mode using the relative abundance of various aluminum and silicon ions.

1. Introduction

Atmospheric aerosols are commonly recognized to have an impact on their environment. Aerosols both directly and indirectly affect climate [1,2], atmospheric chemistry [3], visibility, health [4] and ecosystems such as oceans and vegetation through their participation in biogeochemical cycles [5].

In order to better understand their impact and to identify their sources, many different measurement techniques have been developed to determine size, surface area, volume, hygroscopicity and chemical composition [6]. Aerosol mass spectrometers can simultaneously determine both particle size and chemical composition at the single particle level [6–8]. Within the last decade, aerosol mass spectrometry has become a relatively mature technique even as efforts to reduce size and improve robustness are ongoing. Field measurements are one objective of numerous publications while a second is instrument intercomparisons [9].

Simple compounds such as sulfates, nitrates, sea-salt, metal/metal oxides and halogen-containing particles [10–13] have been extensively studied due to their large abundance and the simplicity of their chemical composition and thus their mass spectra. More recently, quantitation and characterization of organics have received considerable attention [14–16] with increasing interest in high mass compounds [17] and combustion exhaust particles [18,19]. This technique has also been applied to meteoritic aerosols [20,21] and to the identification of bioaerosols [22]. Mineral dusts, on the other hand, have been relatively poorly investigated.

Mineral dust is usually defined as soil-derived particles that do not fit into the previously described classes. Mineral dusts usually contain aluminosilicates, calcium species, and miscellaneous metal oxides. Aerosols of mineral material are important for climate [23] and industry [24]. Mineral dust aerosols, in particular clays, are recognized to affect climate indirectly by heterogeneously nucleating ice at warmer temperatures than required for homogeneous nucleation [25]. Clays, whose major components are phyllosilicates (e.g., montmorrillonite, kaolinite, illite, hectorite, talc), are very efficient in this respect. As an example, montmorrillonite nucleates ice more efficiently than kaolinite [26]. The assessment of such effects requires a better characterization of mineral dust aerosols at a single particle level than what is currently available.

Many authors [27–32] reported on aerosol mass spectrometric analyses of mineral single particles and attempted to classify them. These authors did not attempt to relate mass spectra to a given property or mineralogy, however. The first real step in this direction is the work of Reents and Schabel [33] and Mahadevan et al. [24] who measured the elemental composition of particles such as SiO_2 or Al_2O_3. Whereas elemental composition can pro-

* Corresponding author. Tel.: +41 44 632 72 53; fax: +41 44 633 10 58.
E-mail address: stephane.gallavardin@env.ethz.ch (S. Gallavardin).
[1] Now at Atmospheric Science and Global Change Division, Pacific Northwest National Laboratory, Richland, WA, USA.

1387-3806/$ – see front matter © 2008 Elsevier B.V. All rights reserved.
doi:10.1016/j.ijms.2008.04.031

vide a better description of particles it does not provide speciation information.

Off-line laser mass spectrometric techniques (e.g., LMMS: laser microprobe mass spectrometry) were applied in the last decades for the analysis of mineral samples. They are identical in measurement principle to aerosol mass spectrometers with the exception of the method of presenting the sample to the instrument. In LMMS studies particles collected on a plate are desorbed by the ablation laser. In contrast to this, on-line aerosol mass spectrometers analyse single particles once they are aerodynamically focused into a tight beam and directly introduced into the ion source of the mass analyser. Laser mass spectrometric studies report the feasibility of gaining some speciation and structural information from mineral dusts, such as iron oxides [34,35], calcium species [36,37] and aluminosilicate particles [38–47]. In these studies, the major information source for the elemental speciation or structural information comes from the presence of specific ions and their relative proportions. LMMS has some practical features that are not available in single particle aerosol mass spectrometry that make mineral particle analysis more reliable. For example, the sample quantity can be much larger than a single particle and the laser irradiation conditions are better controlled so that the reproducibility of the measurement is much higher. In on-line single particle laser mass spectrometry, particle information is obtained from a single laser shot with a variable amount of energy on a very small amount of material (e.g., $\sim 10^{-12}$ g for a 1 μm diameter particle of density 2.5 g cm^{-3}). This is due to the inhomogeneous distribution of the energy and the variable location of the particle in the laser beam. Better control of this effect is a contemporary area of research and can be reduced as recently reported by Wenzel and Prather [48] and Steele et al. [49]. The primary advantage of this technique is that these instruments can be mobile. Thus, in situ, real-time and particle preparation-free sampling from diverse platforms such as remote laboratories, ships, and aircraft is possible. This technique also allows the rapid particle size and qualitative chemical analysis of a large number of single particles when compared to LMMS and other single particle mineral analysis methods such as electron microscopy (EM) coupled with X-rays diffraction (XRD) which are more time consuming and not mobile [6]. With this motivation we present a study that is focused on the potential of aerosol single particle mass spectrometry with unipolar detection to differentiate various atmospherically relevant mineral dust particles.

2. Experimental

2.1. Experimental setup

The experimental setup consisted of a dust generator, a cyclone, an Aerodynamic Particle Sizer (APS 3321, TSI Inc., St. Paul, MN) and the particle analysis by laser mass spectrometry (PALMS) instrument. All investigated samples were in the form of a dry powder from the corresponding ground raw material. Powders were further ground if necessary with a mortar such that the final size distribution allowed the particles to be dispersed and sampled by the APS and PALMS instruments (i.e., a sub-micrometer mode size). The powder to be investigated was mechanically aerosolized in a dust generator consisting of a polyethylene bottle vibrated by an electric motor. The motor speed was set such that the aerosol number density produced a mass spectrometer measurement rate of a few Hz. This provided a statistically significant data set while avoiding coincidence effects in the sizing of the particles at high concentrations (i.e., concentrations were never so high that multiple particles were present in the desorption/ionization laser). Dust particles with aerodynamic diameter exceeding 3 μm were removed by an in-line cyclone (Model URG-2000-30ED, URG, Chapel Hill, NC, USA) pumped at 5 lpm by the APS.

The principle and design of the PALMS instrument has been described in the literature, most recently after an upgrade with a timing laser and an aerodynamic lens [50]. Briefly, particles are concentrated and focused into a beam with an aerodynamic lens with near unity transmission for a particle size range 300 nm–2 μm diameter vacuum aerodynamic diameter. At the exit of the aerodynamic lens, particles are accelerated to a terminal velocity that is characteristic of this vacuum aerodynamic diameter. Particles successively cross two laser beams (λ = 532 nm), respectively named the timing and detection lasers, where the particle is detected by its scattered light. The time between detection events and the scattered light amplitude permits the determination of the aerodynamic and geometric diameter and density of the particle [51]. The detection of a particle as it crosses the second laser beam triggers, firing 400 ns later, an excimer laser (λ = 193 nm, ~4 mJ/pulse, ~2.5 ns/pulse, Model PSX-1000, MPB Technology Inc., Quebec, 2001). The excimer laser light (beam size diameter ~150 μm, power density $\sim 10^9$ W/cm^2) ablates the particle and ionizes its constituents. The resulting ions are then analysed using a monopolar reflectron time-of-flight mass spectrometer. Either cations or

Table 1
Product data of the investigated mineral dust aerosols

Dust samples	Origin	Product Notes
Calcium carbonate	Synopharm Schweirhall	
Calcium sulfate	Fluka	
Goethite	Fluka, Ref. 71063 [20344–49]	Natural origin. Contains various amounts of MgO_2, SiO_2, CaO, Al_2O_3
Hectorite	Hectorite SHCa-1 http://www.clays.org/sourceclays/SourceClays.html (January 2007)	Natural origin
Hematite	Synthesized at IMK-FZK Forschungszentrum Karlsruhe, Germany	Trace of chlorine observed with mass spectrometry originates from the hematite synthesis process. Diameter ~0.5 μm
Illite	Arginotec, NX Nanopowder, B + M Nottenkämper, Munich, Germany	77 wt% with 10% kaolinite, 12% calcite
Kaolinite	Fluka, Ref. 03584 [1318-74-7]	Natural origin
Montmorrillonite	Aldrich, K-10, Cat. 28,152-2 [1318-93-0]	Natural origin
Nephelinsyenit	Quarzwerke GmbH, TREMINEX 958-600 EST	57 (vol.%) below 3 μm
Quartzgut	Quarzwerke GmbH, Silmikron VP 795-10/1 ("Quartz Ultrafeinmehl")	99 (wt%) below 2 μm
Silica beads	Palas GmbH, Monosphere 1000	Size 1 or 2 μm
Wollastonite	Quarzwerke GmbH, TREMIN 283-800 EST-M	Treated with Epoxysilane 72 (vol.%) below 4 μm

All minerals listed here except nephelinsyenit, silica beads and wollastonite are minerals of biogeochemical and climatic interest. The later samples were specifically considered to test the methodology presented here.

Table 2
Nominal formula of the investigated minerals [59]

Name	Formula	Class
Calcium carbonate	$CaCO_3$	Carbonate
Calcium sulfate	$CaSO_4$	Sulfate
Goethite	α-$Fe^{III}O(OH)$	Hydroxide
Hectorite	$Na_{0,3}(Mg,Li)_3Si_4O_{10}(OH)_2$	Phyllosilicate
Hematite	α-$Fe^{III}{}_2O_3$	Oxide
Illite	$(K,H_3O)(Al,Mg,Fe)_2(Si,Al)_4O_{10}[(OH)_2,H_2O]$	Phyllosilicate
Kaolinite	$Al_2Si_2O_5(OH)_4$	Phyllosilicate
Montmorrillonite	$(Na,Ca)_{0.33}(Al,Mg)_2Si_4O_{10}(OH)_2.n(H_2O)$	Phyllosilicate
Nephelinsyenit	$(Na,K)AlSiO_4$	Tectosilicate, feldspathoid
Quartz	SiO_2	Tectosilicate
Silica	SiO_2	Tectosilicate
Wollastonite	$CaSiO_3$	Inosilicates

anions can be analysed depending on the polarity of the ion extraction plates.

For each of the investigated dust samples, several hundred to several thousand particles were analysed at each polarity in order to obtain data from a statistically significant set for different laser power levels. Due to the cyclone operation, the APS measurement showed that all investigated samples had a diameter distribution ranging from 0.5 to 3 μm with median sizes from 0.8 to 1.2 μm. The particle background level for a clean and dust-free system was measured before each measurement. In the background, no particles were detected by PALMS.

The samples used in this study, listed in Tables 1 and 2 with their origin and nominal formula, respectively, are mainly minerals of atmospheric and climatic interest according to Claquin et al. [52] and Usher et al. [3]. Samples investigated in this study were chosen to be nominally pure in order to test if materials of similar elemental composition can be differentiated. We do not claim this to be a complete list of all atmospheric dusts. The selection criteria we used were abundance, optical and chemical properties, biogeochemical and climatic impact, and commercial availability. All samples were analysed as they were provided.

2.2. Data analysis

The differentiation of the dust samples was based on the occurrence, abundance or absence, of specific ions of m/z up to 220 and their relative combinations and intensities. Note that all ions are singly charged such that m/z approximately reduces to mass. The investigated ions all relate to the major metal elements constitutive of the material, the corresponding oxides, or the counter species. Mass spectra were first sorted by polarity, particle size and level of laser fluency applied to the particles (i.e., full power or filtered). Mass spectra were then categorized using a C-mean cluster algorithm in different classes that could be manually corrected on a case-by-case basis. Mass spectra for a given class of material (iron oxides, calcium dusts and aluminosilicates) showed similar patterns. Only mass spectra containing ions of the expected material were considered (i.e., unidentified, low ion-abundance or contaminate mass spectra were ignored). These are termed 'informative mass spectra' in the following.

An inventory of the ions, such as iron, calcium, aluminum, silicon, sulfate, and aluminosilicate compounds present in each particle sample was conducted with respect to polarity. The different ions considered in this study are summarized in Table 3. The association of these components in positive and negative mass spectra was then used to determine the elemental composition of the particles. A second pass, if applicable, evaluated the relative abundance of ions for each particle. This was done to assess the possibility of differentiation of mineral dusts while conserving the single particle information. The ion signal ratios were compared for a given size and applied laser power. Selected ion signal ratios were binned, as described in the next section, and a discrimination between samples was made on the basis of one or more ratios. The use of multiple simple ion ratios was used due to the multitude of ions investigated. It was not known, a priori, what ratios were best to identify mineral dusts at the single particle level. As such, only a subset of those ratios are described here (i.e., those ratios which provided the most reliable differentiation information). This approach was preferred to contemporary ones which categorize or cluster single particle mass spectra (e.g., Hinz and Spengler [53] and Rebotier and Prather [54]). Such techniques are often software-specific and mask some single particle information by sorting mass spectra into distinct classes.

Table 3
Typical tracers and their ion m/z assignments for negative and positive mass spectra

Mass spectra	m/z series	Ion assignment
–	12	C
–	16, 17	O, OH
–	44	SiO
–	60, 120, 180	$(SiO_2)_n$: SiO_2, $(SiO_2)_2$, $(SiO_2)_3$
–	76, 136, 196	$(SiO_2)_nO$: $(SiO_2)_2O$, $(SiO_2)_2O$, $(SiO_2)_3O$
–	88, 148	$(SiO_2)_nSi$: $(SiO_2)Si$, $(SiO_2)_2Si$
–	104, 164	$(SiO_2)_nOSi$: $(SiO_2)OSi$, $(SiO_2)_2OSi$
–	116, 176	$X(56)\cdot(SiO_2)_n$: $X\cdot SiO_2$, $X\cdot(SiO_2)_2$ with X = CaO, Si_2
–	56	CaO, Si_2
–	72, 88, 104, 144, 160	Fe_nO_m: FeO, FeO_2, FeO_3, Fe_2O_2, Fe_2O_3 for ^{56}Fe
–	48, 64, 80, 96	SO_x: SO, SO_2, SO_3, SO_4
+	12, 24	C, C_2/Mg
+	40	Ca, tentative: MgO
+	23, 39	Na, K
+	54	^{54}Fe, Al_2
+	56	^{56}Fe, CaO, tentative: MgO_2, Si_2
+	40, 56, 96, 112, 138, 156	Ca_nO_m: Ca, CaO, Ca_2O, $(CaO)_2$, $(CaO)_2$.O for ^{40}Ca

3. Results and discussion

PALMS particle analyses were conducted on the aforementioned compositionally distinct particle types that are all commonly classified as 'mineral dust' by atmospheric scientists. These species – iron oxides, calcium carbonate and sulfate, silica and aluminosilicates – are discussed in detail in the following sections. Fig. 1 presents typical positive and negative ion mass spectra of hematite (a and b), calcium sulfate (c and d) and illite (e and f) which illustrate the radically different spectra produced by these common crustal components. Although it is not surprising that spectrometric separation of these particle types (i.e., hematite from calcium carbonate and illite) is possible based on the simple presence or absence of certain ions it illustrates the diversity within the term "mineral dust". A further challenge, presented in the subsequent sections, is the differentiation of mineral dusts with the same components but different abundances and/or structures.

3.1. Iron minerals

Mass spectra of hematite are presented in Fig. 1 panels a and b. Mass spectra of goethite (not shown here) are very similar to hematite. They are characterized by the occurrence of a strong iron peak at positive m/z = 56 and the related isotopes (m/z = 54, 57, 58).

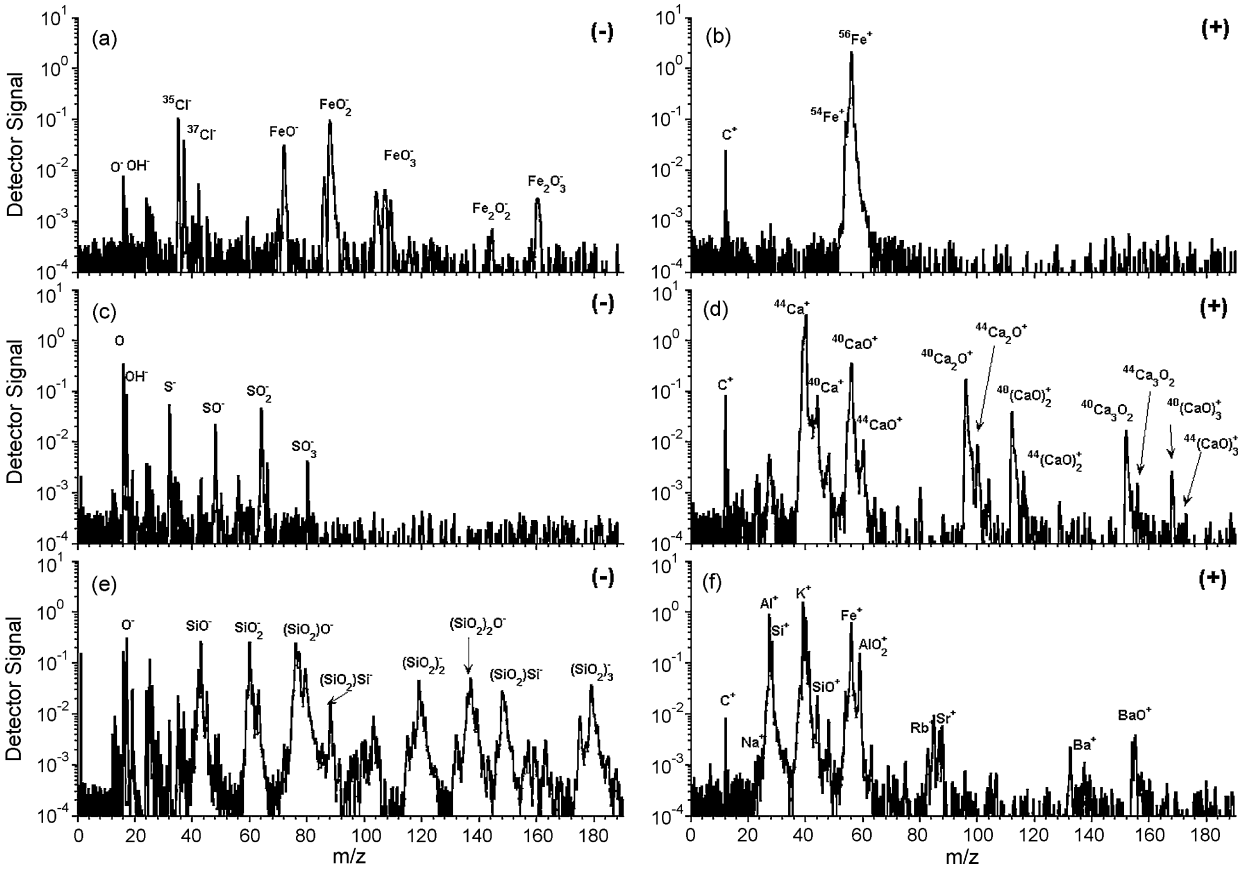

Fig. 1. Typical negative (left panels) and positive (right panels) mass spectra of hematite (a and b), calcium sulfate (c and d), and illite (e and f) obtained by single particle laser desorption/ionization ($\lambda = 193$ nm, $\sim 10^9$ W/cm^2).

Ions such as FeO (72), Fe_2 (112), Fe_2O (128) and Fe_2O_2 (144) were commonly found for low laser power levels ($\sim 5 \times 10^8$ W/cm^2). For negative ions a series of peaks corresponding to FeO (72), FeO_2 (88), FeO_3 (104), Fe_2O_2 (144) and Fe_2O_3 (160) are commonly apparent. It is noteworthy that FeO_3, Fe_2O_2 and Fe_2O_3 ions for goethite were detected in similar proportions as for hematite. The largest ion observed in these mass spectra can therefore not be considered as a reliable determinate for the iron oxide identification.

Positive ions Fe_xO_y found in previous studies of Fe_2O_3 with higher laser wavelengths of $\lambda = 337$ nm [35], 266 and 278.8 nm [34] were also found in our investigation ($\lambda = 193$ nm) but in lesser abundance and occurrence. Our negative mass spectra are consistent with the analysis de Ville d'Avray and co-workers obtained at $\lambda = 337$ nm where the different iron oxide anions FeO, FeO_2, FeO_3, Fe_2O_2 and Fe_2O_3 appeared [35]. The work of Michiels and Gijbels investigated Fe_2O_3 and Fe(O)OH at $\lambda = 266$ nm but only

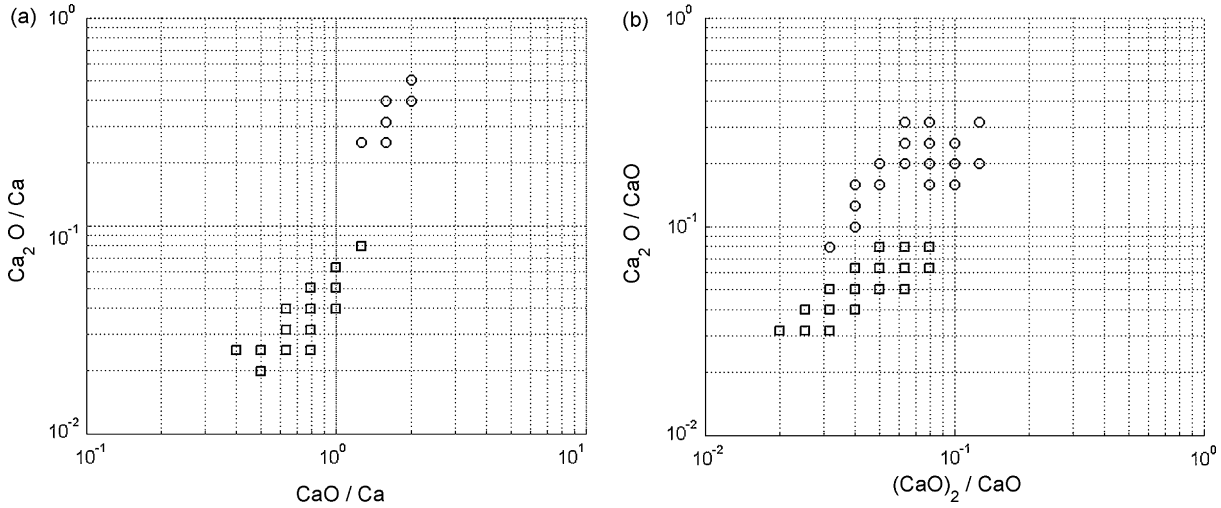

Fig. 2. Pair-wise associated ion signal ratios of selected calcium oxide ions for calcium carbonate (circle) and calcium sulfate (square) from positive ion mode ($\lambda = 193$ nm, $\sim 10^9$ W/cm^2). Each point corresponds to a given binned value of both ratios that contains at least five particles, 90% of which are of the same material, and whose contribution of the ion signal of Ca (a) and CaO (b) exceeded 0.01% of the total ion signal. Each point must also have at least one direct neighbor.

report the observation of positive ions Fe_xO_y without mentioning their respective proportions [55]. Single particle laser mass spectrometry studies of ambient air particles at $\lambda = 337$ nm report the detection of iron oxide positive ions of $m/z = 72$, 88, 112, 128, and 144 assigned to FeO^+, $FeO_2{}^+$, $Fe_2{}^+$, Fe_2O^+, and $Fe_2O_2{}^+$, respectively [56,57]. In some calcium-containing particles, the presence of ions of $m/z = 88$, 128 or 144 indicates that masses 72 and 112 can be assigned to $CaO_2{}^+$ and $(CaO)_2{}^+$ but also to FeO^+ and $Fe_2{}^+$. Silva and co-workers ($\lambda = 266$ nm) report iron only as an elemental peak in positive mode for ambient air particles whereas iron oxide ions, as defined above, were readily observed in negative mode [30]. Finally, the work of Shin and co-workers (at $\lambda = 193$ nm) suggests that the absence of positive Fe_xO_y ions is not linked to the ability of the laser wavelength to produce positive ions from neutral gas-phase species Fe_xO_y [58]. The occurrence of positive iron-containing ions, FeO and Fe_2, was observed in this study when the particles were irradiated with a lower laser power than in the cases where only atomic iron was present in the mass spectra. This suggests that positive mass spectra of iron oxide species depend on the laser light characteristics.

Since pure iron oxide particles are composed of iron, oxygen, and hydrogen for goethite, the only way to differentiate the sample is to compare the relative occurrence of the iron oxide ions for a given particle size and laser power level. This approach could not be performed in this study because the size distribution of the hematite and the goethite powders did not overlap. Moreover, neither sample was pure and this may affect the behaviour of the ion signal ratios. Hematite was found to contain chlorine (as a by-product of the production process) which may affect the iron oxides ion signal ratios. This is likely due to the fact that Cl has a higher electron affinity (3.6 eV) than the iron oxides FeO_y (1.5–3.3 eV). Goethite was found to contain aluminosilicate materials which may affect the iron oxides ion signal ratios in a different manner. Despite the limitations imposed by the samples iron was detectable in both positive and negative ion mode. The presence of iron oxides was more clear in negative than in positive ion mode. Speciation of iron oxides will require future work with high-purity samples in an overlapping size range.

3.2. Calcium minerals

Mass spectra of calcium sulfate are presented in Fig. 1 panels c and d. Positive mass spectra of calcium carbonate, calcium sulfate and wollastonite are marked by the presence of calcium in an unassociated form as well as by the series of calcium oxides, Ca_nO_n and Ca_mO_{m-1} with $n = 1$–3 and $m = 2$–3, for the two most abundant calcium isotopes (^{40}Ca and ^{44}Ca). In the case of wollastonite, silicon was also detected in positive ion mode. In the case of calcium sulfate, the presence of sulfate ions was rarely found in positive polarity. Conversely, the negative ion mode provided information related to the counter-ions, i.e., the species associated with the calcium atom. Typical signatures included SO (48), SO_2 (64), SO_3 (80) and SO_4 (96) for calcium sulfate or SiO_2 (60) and $(SiO_2)O$ (76) for wollastonite. For calcium carbonate, negative mass spectra did not provide information to unambiguously identify the particle material since no ions of $m/z = 28$, 44 or 60 related to CO, CO_2 or CO_3 were detected. Instead, only carbon C (12) and oxygen O (16) were apparent.

LMMS studies agree with these observations for $CaCO_3$ and $CaSO_4$ [36]. The observed signature of two positive ion series, Ca_nO_n and Ca_nO_{n-1}, for calcium-rich material in positive ion mode is supported by Struyf et al. [37] and by aerosol mass spectrometric field measurements [29,32]. Not investigated in this study, a similar pattern has also been found for calcium nitrate $Ca(NO_3)_2$ [37].

Table 4
Identification rates of the Ca-dust based on selected calcium oxide ion signal ratios using positive mass spectra

		Condition 1[a] $\sim 10^9$ W/cm^2 (%)	Condition 2[b] $\sim 5 \times 10^8$ W/cm^2 (%)
(Ca_2O)/Ca vs. CaO/Ca	$CaCO_3$	15	72.6
	$CaSO_4$	46.6	5.5
$(CaO)_2$/Ca vs. CaO/Ca	$CaCO_3$	7.1	50.7
	$CaSO_4$	17.8	–
(Ca_2O)/CaO vs. $(CaO)_2$/CaO	$CaCO_3$	46	79.1
	$CaSO_4$	69.1	8.1

[a] In Condition 1, 452 and 548 MS were recorded for $CaCO_3$ and $CaSO_4$, respectively.
[b] In Condition 2, 2058 and 1017 MS were recorded for $CaCO_3$ and $CaSO_4$, respectively.

Fig. 2 reports the values of selected calcium oxide ion signal ratios that lead to the differentiation of calcium carbonate from calcium sulfate. Table 4 reports the probability of identifying calcium carbonate and calcium sulfate. Using calcium oxide ions, calcium carbonate can be differentiated from calcium sulfate for 79 and 46% of the particles for the respective laser power $\sim 5 \times 10^8$ and 10^9 W/cm^2. Under similar conditions, calcium sulfate can be differentiated from calcium carbonate for 8–69% of the particles. The different behaviour with respect to laser power is noteworthy. This is likely due to the ionization potential of the investigated material. In this case the more difficult to ionize sulfates require the higher power.

The presence of calcium can be determined, on a single particle basis, in positive ion mode. The speciation of calcium is possible by association in negative ion mode for calcium sulfate and calcium silicate. It is also often possible to differentiate calcium sulfate and calcium carbonate based on the relative occurrence of calcium oxide ions.

3.3. Silicon minerals

3.3.1. Pure silica particle beads and industrial quality quartz (SiO_2) particles

Samples of "industrial quality" quartz and silica beads were analysed with the PALMS instrument but only a few mass spectra with ion signals corresponding to silicon material were obtained. It proved difficult to produce informative mass spectra in either positive or negative ion mode from pure silica or quartz samples even though particles were detected optically with high efficiency. The absence of informative mass spectra for pure/quasi-pure silica material is due to both the chemical composition (in particular, the strong cohesion of the material) and insufficient desorption/ionization laser power incident on the particle surface. This is confirmed by the fact that the particle size met the criteria for the desorption/ionization laser to be triggered at the correct time and by the fact that less pure particles of 'industrial quality' (98.5% SiO_2, 1.0% Al_2O_3, 0.1% of CaO + MgO and 0.1% of $Na_2O + K_2O$) did produced mass spectra at a higher rate. For silica beads, no informative mass spectra were observed over hundreds of particles optically detected whereas industrial quartz and phyllosilicates particles produced informative mass spectra in positive ion mode under identical conditions. This theory is further supported by comparing the mean applied power density used in this work ($\sim 10^9$ W/cm^2, the highest achievable in the present study) with the results of Reents and co-workers who obtained mass spectra of silica but with a one order of magnitude higher laser power ($\sim 10^{10}$ W/cm^2) [27,33].

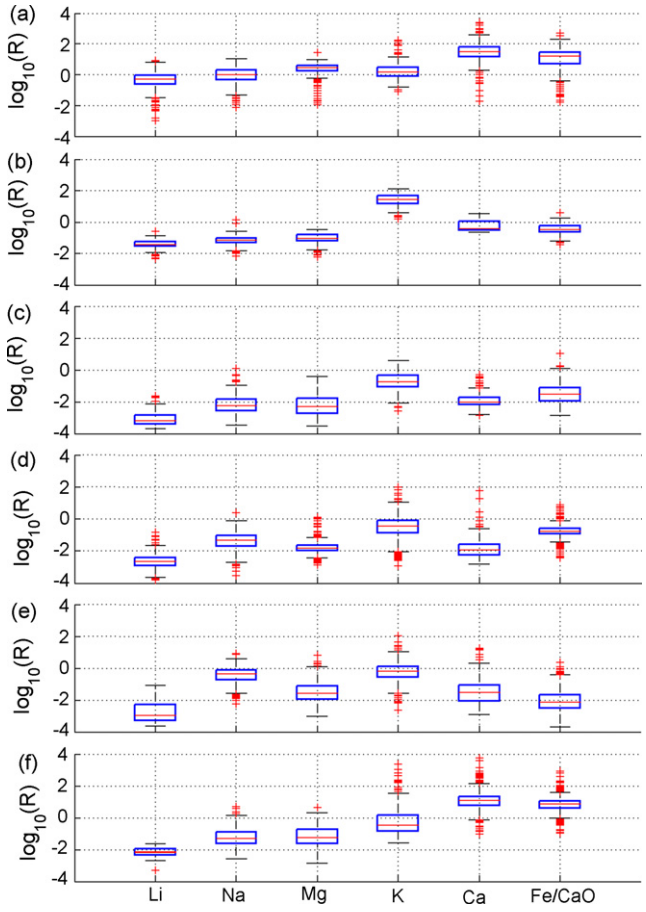

Fig. 3. Distribution of the ratio *R* of the ion signal of a given element (Li, Na, Mg, K, Ca and Fe/CaO) to the total ion signal of Al and Si from positive ion mode (λ = 193 nm, ~10^9 W/cm^2) for (a) hectorite (349 MS), (b) illite (560 MS), (c) kaolinite (344 MS), (d) montmorrillonite (766 MS), (e) nephelinsyenit (606 MS), and (f) wollastonite (622 MS). Note the high ratio for potassium in all aluminosilicate dusts. The top and bottom of the box indicate the upper and lower quartile values of $\log_{10}$(R). The line inside the box reports its mean value. The whiskers report the range over which span the adjacent values. Crosses beyond the whiskers indicate the values of the remaining ratio values.

3.3.2. *Aluminosilicates*

Aluminosilicates are complex compounds in terms of both structural and elemental composition. Fig. 1 panels e and f illustrate this for illite particles. The different samples studied in this work contain essentially the same elements (O, Si, Al, K, Ca, Na, Mg, Fe and Li) in various quantities, as illustrated in Table 2. Fig. 3 reports for each aluminosilicate species the distribution of the ratio of the ion signal Li, Na, Mg, K, Ca, Fe to the total ion signal of aluminum and silicon. Elements appeared in their un-associated form. Aluminum, silicon, calcium and iron also appeared as oxides. For iron-free and Ca- or Mg-rich particles (montmorrillonite and hectorite), an ion peak at m/z = 56 was frequently observed and this was attributed to CaO^+ and/or MgO_2^+. The ion of m/z = 56 found in Ca, Mg, and Fe poor material, e.g., kaolinite, is attributed to Si_2^+. Hectorite, a Ca-free material, present a strong signal for ions of m/z = 40, which is attributed to MgO^+. The absolute identification of the ions at m/z = 56 as Fe using the ^{54}Fe isotope may not always be appropriate since, in aluminum-rich particles such as gibbsite ($Al(OH)_3$), ions of m/z = 54 can also be attributed to Al_2^+. Frequently other elements, such as rubidium (Rb, 85), strontium (Sr, 88), barium (Ba, 138) and lead (Pb, 208) and occasionally some of their oxides (e.g., BaO (154)) were observed in different combinations, representing at times up to 85% of the ion signal. According to the formulas of the studied aluminosilicates, these should be considered as minor elements and will, for this reason, be ignored in the remainder of this study. Their sporadically high abundance is likely due to their low ionization potential when compared to some of the major elements (e.g., silicon, magnesium and iron). It is noted that positive mass spectra were generally easier to obtain than negative ones. It is also noted that silicon oxide ions, such as $M_lSi_nO_m^+$ (with M = Be, Mg, Al, K, Ca, Mn, Fe, Zr), reported by Tsugoshi and coworkers for kaolinite and wollastonite [38] were not observed in this work.

Fig. 3 shows that differentiation using positive mass spectra is possible for all the silicon-containing species. Hectorite appears to be well defined due to a large fraction of lithium, sodium and magnesium (detected as MgO^+ (40) and MgO_2^+ (56)). Illite is identified by a K/(Al,Si) ratio of ~26, larger than for all other samples. Kaolinite can be identified by a low ion signal of all non-aluminum and silicon metals when compared to the other aluminosilicate samples. Nephelinsyenit is identified by a large ion signal ratio of Na and K with respect to Al + Si. Finally, wollastonite can be identified by the large proportion of Ca and CaO ions compared to Na, Mg, and K. The identification of montmorrillonite was less clear, in large part

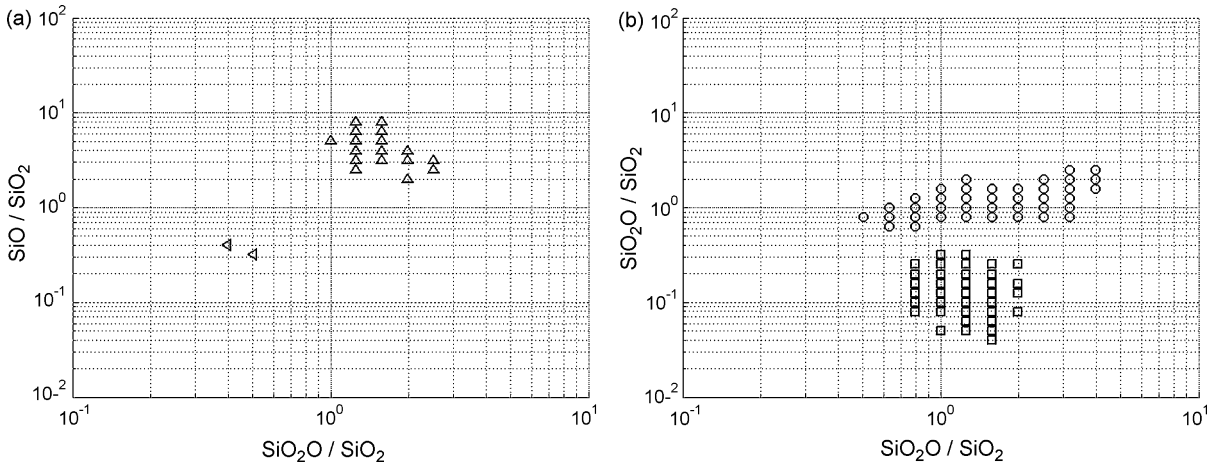

Fig. 4. Pair-wise associated ion signal ratio of selected silicon oxide ions for (a) hectorite (up triangle), wollastonite (left triangle), (b) illite (circle), and montmorrillonite (square) from negative ion mode (λ = 193 nm, ~5×10^8 W/cm^2). Each point corresponds to a given binned value of both ratio that contains at least five particles, 90% of which are of the same material, and whose contribution of the ion signal of SiO_2 exceed 0.01% of the total ion signal. Each point must also have at least one direct neighbor.

Table 5
Identification rates of aluminosilicate particles based on selected silicon oxide ion signal ratios using negative mass spectra

		Condition 2 $\sim 5 \times 10^8$ W/cm^2	Number of MS for which both ratios are defined	Number of MS with SiO_2
SiO/SiO_2 vs. $SiO_2 \cdot O/SiO_2$	Hectorite	48.6%	455	969
	Wollastonite	9.3%	668	1134
SiO/SiO_2 vs. $SiO_2.O/SiO_2$	Montmorrillonite	86.3%	2085	2202
	Illite	67.9%	2876	3335

due to the unexpectedly large signal due to potassium. The same conclusions can be drawn when the laser power was reduced to $\sim 5 \times 10^8$ from $\sim 10^9$ W/cm^2. It is noteworthy that potassium was frequently found at high abundance compared to aluminum and silicon for all mineral samples. This can be explained by its low ionization potential (4.3 eV), the lowest of all detected ions found in the mineral dusts of this study. As such, we suggest that the abundance of potassium be used as an auxiliary, not primary, criterion for the speciation of mineral dust. Indeed, even under the controlled conditions of this study up to 20% of the spectra did not contain abundant Si or Al ions but either potassium, iron or barium. For these mass spectra, it was not possible to definitively attribute them to aluminosilicate particles but only to assign them a mineral origin. Further complicating this is that biogenic material would also be expected to contain potassium and sodium in significant abundance although the presence of organic material and phosphorous would likely differentiate such a spectrum. The presence of easy-to-ionize and trace elements thus makes the identification of aluminosilicates using positive mass spectra more difficult.

Negative mass spectra proved more difficult to obtain and less sensitive to the elemental composition. Indeed, all negative mass spectra of the aluminosilicate particles are similar since they are the sum of variable contributions of the same silicon and aluminum oxide ion clusters (see Fig. 1 for illite). In negative mode the main peaks can be assigned to ionic species with a aluminum-silicon 'skeleton' such as $(SiO_2)_nXY$, with $n = 0$–3, X = AlO_2, AlOH and Y = O, OH, Si, SiO, SiOH, Si_2, CaO, MgO_2 or Fe. The occurrence of similar ion clusters from aluminosilicate minerals is also reported in aerosols [32] and off-line laser mass spectrometric studies [41–43,46,47]. The presence of such ions is enhanced by the frequent replacement of silicon by aluminum in the material and the greater electron affinity of AlO_2 than SiO_2 (~4 eV versus 2.76 eV) [42]. These ion clusters can be used as 'tracers' for sample differentiation given particles of similar sizes and similar levels of laser power. Candidate tracers are defined in Table 3. For example, silicon oxide ion clusters of m/z = M ($(SiO_2)_n$, $(SiO_2)_nO$, $(SiO_2)_nSi$, $(SiO_2)_nOSi$, $X(56)\cdot(SiO_2)_n$), the corresponding clusters with a silicon atom exchanged by an aluminum atom (m/z = M−1), and the clusters with an additional hydrogen atom (m/z = M+1) can be used. The above-defined tracers are labelled for simplicity in the following and in Fig. 4 as if they were only silicon oxide ion clusters and having a m/z of M.

Fig. 4 presents the relationship between ion signal ratios SiO/SiO_2 and $SiO_2.O/SiO_2$. These were chosen because these ions were the most frequently detected for all the aluminosilicates dusts at both laser power levels. This approach is presented for the pairs of mineral dusts hectorite, wollastonite and illite, montmorrillonite for which the particle size and laser power level allowed for comparison. At low laser power ($\sim 5 \times 10^8$ W/cm^2), hectorite can be differentiated from wollastonite in 48 and 9% of the mass spectra where SiO_2^- was detected, respectively. Montmorrillonite and illite can likewise be differentiated from each other in 86 and 68% of the mass spectra where SiO_2^- is detected, respectively (Table 5). Fig. 4b illustrates the need to consider a second ion signal ratio, SiO/SiO_2, to discriminate illite and montmorrillonite since these samples cannot be differentiated given an overlapping ion signal ratio for SiO_2O/SiO_2. The distinction between aluminosilicates material thus is partially possible using aluminum and silicon oxide ions. It should be noted that, depending on the sample, negative mass spectra with only O, OH, and sometimes associated with organics and sulfates comprised up to 25% of the mass spectra. These mass spectra could not be unambiguously attributed to aluminosilicate particles and contribute to the low level of differentiation.

In summary, the elemental composition and differentiation of aluminosilicates was possible in positive ion mode. This was complicated in a fraction of the cases by the presence of easy-to-ionize substances of low abundance. Negative ion mode provided a complementary approach which was less sensitive to trace elements but for which a fraction of particles did not produce mass spectra with sufficient ions to allow differentiation.

4. Conclusions

This study presents the use of the PALMS instrument to analyse and differentiate mineral particles consisting of iron oxides, calcium materials, and aluminosilicate compounds both on-line and at a single particle level. This study is not meant to specifically translate to all other single particle mass spectrometers. Instead, it is meant to indicate the ability of such instruments to perform differentiation among materials which are normally combined into a single category despite the fact that they have very different properties with respect to climate, human health, atmospheric chemistry, and biogeochemical cycles. Indeed, the vast amount of single particle spectra that have been and will be obtained can utilize this type of differentiation.

It is shown that in positive ion mode the qualitative elemental composition for the species Na, Mg, Al, Si, K, Ca, Fe, Li, Rb, Sr, Ba, and Pb can be inferred for at least 80% of the particles that produced a mass spectrum. With the exception of the calcium-containing samples, negative ion mode is not necessary to differentiate the mineral dusts in this study. Differentiation of the calcium dusts required the identification of the counter-ions (sulfates and silicates) and this required negative ion mode. Carbonates could, at least partially, be defined using only positive polarity.

The relative abundance of the oxide ions of the key metals of the mineral dusts often allowed for element speciation in positive and negative ion mode for calcium and aluminosilicate material, respectively. For example, a fraction of calcium carbonate and calcium sulfate particles could be differentiated using only calcium oxide ion abundance. Similarly, hectorite, wollastonite, illite, and montmorrillonite could often be differentiated using only aluminum and silicon oxide ions. The presence of impurities and the different particle sizes restricts this level of analysis for the iron oxide particles investigated here.

With the exception of the calcium-containing mineral dusts differentiation was possible using either polarity. For the other species elemental information was provided by positive polarity ions whereas structural information was given by negative ions. Thus, a dual polarity mass spectrometer is preferred but not absolutely required for this type of differentiation.

The samples used in this study were nominally pure whereas real atmosphere samples are complex mixtures. Examples include calcium carbonate particles from deserts converted by aging to calcium sulfate or/and nitrate or internal and external mixtures of different clays such as illite, montmorrillonite, and kaolinite. Further, real atmospheric particles are often processed by water and acidic gases which may also influence the response in single particle mass spectrometers. As such, future studies will need to focus on differentiation of real-world materials.

In addition to future studies using higher purity samples and those of atmospheric origin there are other follow-on studies that would be productive. First, there have been recent efforts by several single particle mass spectrometry groups to use separate lasers for ablation and ionization. Such a 'two-step' scheme may provide an improvement over the level of differentiation shown here if it is possible to tune the wavelengths and fluences to refractory particles. A second approach gaining recent attention that bears consideration is to compliment a single particle instrument with spectral and/or electron scattering methods in order to gain information on the elements speciation and material mineralogy.

Acknowledgements

The authors gratefully acknowledge the designers and developers of the PALMS instrument, Daniel M. Murphy and David S. Thomson. We thank NOAA for the loan of the laboratory PALMS instrument for these studies and Ottmar Moehler and the AIDA facility for providing mineral dust samples and advice. We acknowledge Quarzwerke GmbH, Germany for providing the silicate samples. Finally, we thank ACCENT, ETH-Zurich, and PNNL LDRD for the funding to sponsor this study.

References

[1] Intergovernmental Panel on Climate Change Climate Change 2001: The Scientific Basis, Cambridge University Press, Cambridge, 2001.
[2] U. Lohmann, J. Feichter, Atmos. Chem. Phys. Discuss. 5 (2005) 715.
[3] C.R. Usher, A.E. Michel, V.H. Grassian, Chem. Rev. 103 (2003) 4883.
[4] C.I. Davidson, R.F. Phalen, P.A. Solomon, Aerosol Sci. Technol. 39 (2005) 737.
[5] D.A. Grantz, J.H.B. Garner, D.W. Johnson, Environ. Int. 1006 (2003) 1.
[6] P.A. Baron, K. Willeke (Eds.), Aerosol Measurement: Principles, Techniques and Applications, 2nd ed., Wiley-Interscience, New York, 2001.
[7] D.T. Suess, K.A. Prather, Chem. Rev. 99 (1999) 3007.
[8] R.C. Sullivan, K.A. Prather, Anal. Chem. 77 (2005) 3861.
[9] A.M. Middlebrook, D.M. Murphy, S.-H. Lee, D.S. Thomson, K.A. Prather, R.J. Wenzel, D.-Y. Liu, D.J. Phares, K.P. Rhoads, A.S. Wexler, M.V. Johnston, J.L. Jimenez, J.T. Jayne, D.R. Worsnop, I. Yourshaw, J.H. Seinfeld, R.C. Flagan, J. Geophys. Res. 108 (2003) 8413, doi:10.1029/2001JD000660.
[10] D.M. Murphy, D.S. Thomson, A.M. Middlebrook, M.E. Schein, J. Geophys. Res. 103 (1997) 16485.
[11] D.M. Murphy, D.S. Thomson, J. Geophys. Res. 102 (1997) 6341.
[12] D.M. Murphy, D.S. Thomson, J. Geophys. Res. 102 (1997) 6353.
[13] D.M. Murphy, D.S. Thomson, A.M. Middlebrook, Geophys. Res. Lett. 24 (1997) 3197.
[14] P.J. Silva, K.A. Prather, Anal. Chem. 72 (2000) 3553.
[15] B.D. Morrical, D.P. Fergenson, K.A. Prather, J. Am. Soc. Mass Spectrom. 9 (1998) 1068.
[16] B.W. LaFranchi, J. Zahardis, G.A. Petrucci, Rapid Commun. Mass Spectrom. 18 (2004) 2517.
[17] D.S. Gross, M.E. Gälli, M. Kalberer, A.S.H. Prevot, J. Dommen, M.R. Alfarra, J. Duplissy, K. Gaeggeler, A. Gascho, A. Metzger, U. Baltensperger, Anal. Chem. 78 (2006) 2130.
[18] P.J. Silva, K.A. Prather, Environ. Sci. Technol. 31 (1997) 3074.
[19] M.R. Canagaratna, J.T. Jayne, D.A. Ghertner, S. Herndon, Q. Shi, J.L. Jimenez, P.J. Silva, P. Williams, T. Lanni, F. Drewnick, K.L. Demerjian, C.E. Kolb, D.R. Worsnop, Aerosol Sci. Technol. 38 (2004) 555.
[20] D.M. Murphy, D.S. Thomson, T.M.J. Mahoney, Science 282 (1998) 1664.
[21] D.J. Cziczo, D.S. Thomson, D.M. Murphy, Science 291 (2001) 1772.
[22] D.P. Fergenson, M.E. Pitesky, H.J. Tobias, P.T. Steele, G.A. Czerwieniec, S.C. Russell, C.B. Lebrilla, J.M. Horn, K.R. Coffee, A. Srivastava, S.P. Pillai, M.-T.P. Shih, H.L. Hall, A.J. Ramponi, J.T. Chang, R.G. Langlois, P.L. Estacio, R.T. Hadley, M. Frank, E.E. Gard, Anal. Chem. 76 (2004) 373.
[23] C.S. Zender, R.L. Miller, I. Tegen, EOS 85 (48) (2004) 509.
[24] R. Mahadevan, D. Lee, H. Sakurai, M.R. Zachariah, J. Phys. Chem. A 106 (2002) 11083.
[25] H.R. Pruppacher, J.D. Klett, Microphysics of Clouds and Precipitation, 2nd ed., Kluwer Academic Publishers, The Netherlands, 1997.
[26] A. Salam, U. Lohmann, B. Crenna, G. Lesins, P. Klages, D. Rogers, R. Irani, A. MacGillivray, M. Coffin, Aerosol Sci. Technol. 40 (2006) 134.
[27] W.D. Reents, S.W. Downey, A.B. Emerson, A.M. Mujsce, A.J. Muller, D.J. Siconolfi, J.D. Sinclair, A.G. Swanson, Aerosol Sci. Technol. 23 (1995) 263.
[28] A. Trimborn, K.-P. Hinz, H. Iglseder, M. Greweling, B. Spengler, J. Aerosol Sci. 29 (Suppl. 1) (1998) S883.
[29] P.J. Silva, R.A. Carlin, K.A. Prather, Atmos. Environ. 34 (2000) 1811.
[30] S. Owega, G.J. Evans, R.E. Jervis, J. Tsai, M. Fila, P.V. Tan, Environ. Pollut. 120 (2002) 125.
[31] S.-H. Lee, D.M. Murphy, D.S. Thomson, A.M. Middlebrook, J. Geophys. Res. 107 (2002) 4003, doi:10.1029/2000JD000011.
[32] R.C. Sullivan, S.A. Guazzotti, D.A. Sodeman, K.A. Prather, Atmos. Chem. Phys. Discuss. 6 (2006) 4109.
[33] W.D. Reents, M.J. Schabel, Anal. Chem. 73 (2001) 5403.
[34] B. Maunit, A. Hachimi, P. Manuelli, P.J. Calba, J.F. Muller, Int. J. Mass Spectrom. Ion Process. 156 (1996) 173.
[35] A.T. de Ville d'Avray, E.E. Carpenter, C.J. O'Connor, R.B. Cole, Eur. J. Mass Spectrom. 4 (1999) 441.
[36] F.J. Bruynseels, R.E. Van Grieken, Spectrochim. Acta 38B (1983) 853.
[37] H. Struyf, L. Van Vaeck, K. Poels, R. Van Grieken, J. Am. Soc. Mass Spectrom. 9 (1998) 482.
[38] T. Tsugoshi, T. Kikuchi, K. Furuya, Y. Ino, Y. Hayashi, Mikrochim. Acta 3 (4-6) (1991) 125.
[39] S. Jeong, K.J. Fisher, R.F. Howe, G.D. Willett, Micropor. Mater. 4 (1995) 467.
[40] C. Xu, L. Wang, S. Qian, L. Zhao, Z. Wang, Y. Li, Chem. Phys. Lett. 281 (1997) 426.
[41] C. Xu, Y. Long, R. Zhang, L. Zhao, S. Qian, Y.Y. Li, Appl. Phys. A 66 (1998) 99.
[42] C. Xu, Y. Long, S. Qian, Y. Li, Micropor. Mesopor. Mater. 39 (2000) 351.
[43] P.E. Lafargue, J.J. Gaumet, J.F. Muller, Chem. Phys. Lett. 288 (1998) 494.
[44] P.E. Lafargue, J.J. Gaumet, J.F. Muller, A. Labrosse, J. Mass Spectrom. 31 (1996) 623.
[45] J.M. Beusen, P. Surkyn, R. Gijbels, F. Adams, Spectrochim. Acta 38B (1983) 843.
[46] E. Erel, F. Aubriet, G. Finqueneisel, J.-F. Muller, Anal. Chem. 75 (2003) 6422.
[47] J. Castello, J.J. Gaumet, J.-F. Muller, G. Friour, J. Guilment, O. Poncelet, Prog. Solid State Chem. 34 (2006) 95.
[48] R.J. Wenzel, K.A. Prather, Rapid Comm. Mass. Spectrom. 28 (2004) 1525.
[49] P.T. Steele, H.J. Tobias, D.P. Fergenson, M.E. Pitesky, J.M. Horn, G.A. Czerwieniec, S.C. Russell, C.B. Lebrilla, E.E. Gard, M. Frank, Anal. Chem. 75 (2003) 5480.
[50] D.J. Cziczo, D.S. Thomson, T.L. Thompson, P.J. DeMott, D.M. Murphy, Int. J. Mass Spectrom. 258 (1–3) (2006) 21.
[51] D.M. Murphy, D.J. Cziczo, P.K. Hudson, M.E. Schein, D.S. Thomson, J. Aerosol Sci. 35 (2004) 135.
[52] T. Claquin, M. Schulz, Y.J. Balkanski, J. Geophys. Res. 104 (1999) 22243.
[53] K.-P. Hinz, B. Spengler, J. Mass. Spectrom. 42 (2007) 843.
[54] T.P. Rebotier, K.A. Prather, Anal. Chim. Acta 585 (2007) 38.
[55] E. Michiels, R. Gijbels, Anal. Chem. 56 (1994) 1115.
[56] A. Held, K.-P. Hinz, A. Trimborn, B. Spengler, O. Klemm, J. Aerosol Sci. 33 (2002) 581.
[57] K.-P. Hinz, A. Trimborn, E. Weingartner, S. Henning, U. Baltensperger, B. Spengler, J. Aerosol Sci. 36 (2005) 123.
[58] D.N. Shin, Y. Matsuda, E.R. Bernstein, J. Chem. Phys. 120 (9) (2004) 4157.
[59] http://webmineral.com, January 2007.